Collision Avoidance Predictive Motion Planning Based on Integrated Perception and V2V Communication

Shiyao Zhang, *Member, IEEE*, Shuai Wang, *Member, IEEE*, Shuai Yu, *Member, IEEE*, James J. Q. Yu, *Senior Member, IEEE*, and Miaowen Wen, *Senior Member, IEEE*

***Abstract*— Autonomous vehicles (AVs), as one of the cores in future intelligent transportation systems (ITSs), can facilitate reliable and safe traffic operations and services. The ability to automatically perform effective AV motion planning and deploy efficient perception systems is vital for advancing the quality of core transportation services. However, existing research studies have only considered the applications of either of these approaches, which neglect their necessary interactions in real-world AV motion planning systems. To address this problem, we design an AV motion planning strategy based on motion prediction and V2V communication. Specifically, we propose the perception system and V2V communication module to provide real-time traffic and vehicular information to the participated AVs. Then, we formulate the AV lane-change motion planning problem through the scope of model predictive control based problem, as well as proposing the method on learning optimal motion planning by means of a novel deep learning technique. We conduct extensive case studies to evaluate the performance of the proposed system model. Our experimental results demonstrate the effectiveness of the proposed system model under various traffic conditions. In addition, the robustness of the perception system is guaranteed by utilizing the Car Learning to Act (CARLA) system with available V2V communication.**

Manuscript received July 26, 2021; revised January 15, 2022 and April 2, 2022; accepted April 25, 2022. This work was supported in part by the General Program of Guangdong Basic and Applied Basic Research Foundation under Grant 2021KQNCX078, in part by the Open Research Fund from Guangdong Laboratory of Artificial Intelligence and Digital Economy [Shenzhen (SZ)] under Grant GML-KF-22-17, in part by the Shenzhen Industrial Application Projects of Undertaking the National Key Research and Development Program of China under Grant CJGJZD20210408091600002, and in part by the Guangdong Basic and Applied Basic Research Project under Grant 2021B1515120067. The Associate Editor for this article was A. Jolfaei. *(Corresponding authors: Shuai Wang; James J. Q. Yu.)*

Shiyao Zhang is with the Academy for Advanced Interdisciplinary Studies, Southern University of Science and Technology, Shenzhen 518055, China, and also with the Guangdong Laboratory of Artificial Intelligence and Digital Economy (SZ), Shenzhen 518060, China (e-mail: syzhang@ieee.org).

Shuai Wang is with the Guangdong-Hong Kong-Macao Joint Laboratory of Human-Machine Intelligence-Synergy Systems, Shenzhen Institute of Advanced Technology, Chinese Academy of Sciences, Shenzhen 518055, China, and also with the Guangdong Laboratory of Artificial Intelligence and Digital Economy (SZ), Shenzhen 518060, China (e-mail: s.wang@siat.ac.cn).

Shuai Yu is with the School of Computer Science and Engineering, Sun Yat-sen University, Guangzhou 510275, China (e-mail: yushuai@mail.sysu.edu.cn).

James J. Q. Yu is with the Department of Computer Science and Engineering, Southern University of Science and Technology, Shenzhen 518055, China (e-mail: yujq3@sustech.edu.cn).

Miaowen Wen is with the School of Electronic and Information Engineering, South China University of Technology, Guangzhou 510641, China (e-mail: eemwwen@scut.edu.cn).

Digital Object Identifier 10.1109/TITS.2022.3173674

***Index Terms*— Autonomous vehicles, car learning to act system, intelligent networked vehicle systems, motion planning, perception system, V2V communication.**

I. Introduction

IN RECENT years, an intelligent transportation system (ITS) has emerged as a promising technology in a smart city. Through information processing and communication technologies, ITS can function the city transportation system productively, which improves the quality of core transportation operations and services [1]. Autonomous vehicles (AVs), as one of the essential components in ITS, are capable of operating without human involvement while sensing their surrounding environment. Approximately 81% of annual vehicle-involved crashes can be greatly mitigated based on AV techniques, according to the Research and Innovative Technology Administration (RITA) of the U.S. Department of Transportation (USDOT) [2]. Hence, the maturing technology in AVs has the potential to enhance the safety, efficiency, and convenience of ITS, such as the efficient autonomous intersection management in urban road networks [3].

Due to the development of AV technology, the control strategies of AVs have become a hot research topic in current years. Several studies have investigated the motion planning strategies of AVs in ITS. For instance, [4] studied the state of the art on motion planning and control algorithms by using AVs. The motion planning strategies developed in [5]–[9] lead to optimizing the AV travel path or trajectory on various roads by tracking the low-level feedback controller. Besides, the continuous path of AVs can be obtained through proper lane-change motion strategies [10]–[15]. Hence, the use of optimal AV motion planning approaches can bring substantial capabilities for providing timely and safe operations in ITS.

When considering the utilization of AV motion planning methods, the intelligent networked vehicle system (INVS) can help sense the surrounding environment to complete the local navigational tasks. This system refers to the use of dynamic map fusion techniques in AV cooperative perception, motion planning, and maneuvering tasks [16], [17]. These techniques are classified into three levels, namely, data level [18], feature level [19], and object-level [20]. The data-level and feature-level approaches can easily incur high communication overheads and most object-level methods do not

consider the sensing and model uncertainties. To tackle these issues, a dynamic map fusion framework with Car Learning to Act (CARLA) system was proposed in [21], [22]. This system enables scored-based object-level fusion and deploys a distributed online learning method, which leads to low communication overhead and high map quality.

Besides, the feasibility of INVS depends on the availability of vehicle-to-vehicle (V2V) communication. In practice, reliable wireless communications serve a crucial role in facilitating daily social activities [23], [24]. V2V communication systems enable efficient wireless transmission among AVs, which further facilitates safe and effective traffic operations and services in ITS. These systems can provide each AV with the real-time movement information of other nearby AVs equipped with V2V techniques within the communication range. The study in [25] demonstrated the importance of the perception system concerning V2V communication systems. Existing studies have investigated implementing V2V communication into the perception system, e.g. [26]–[28]. However, the incorporation of real-time AV motion planning with these systems is neglected. Therefore, it is a pressing issue on how to implement real-time motion planning on these systems.

To bridge the research gaps, an AV motion planning strategy framework, which consists of motion prediction and V2V communication, is proposed in this paper. In this framework, we focus on how to develop a framework to enable the perception system to adaptively generate real-time information to cope with the AV motion planning strategy. In addition, the map quality and V2V communication overhead can be improved by considering the online learning model. This promotes the utilization of the perception system with V2V communication techniques in practice. Then, we emphasize investigating how to operate the effective lane-change motion for the ego AV, which considers the safety, speed, and traffic rules. In the meantime, the AV participated in the process of motion planning can interact with the perception system in real-time. The implementation of learning optimal planning helps the ego AV to adjust the lane-change motion plans under real-time traffic conditions.

The main contributions of this research work can be summarized as follows:

- We develop a vision perception system framework to learn both semantic and geometry information of the environment, in order to conduct a timely interaction between the system and real-time motion planning. This framework is more general and practical than the existing ones since the dynamic real-time motion planning approach is developed within the feasible regions.
- We formulate a motion planning problem based on model predictive control (MPC) for the ego AV, in order to determine the optimal lane-change motion based on the availability of the perception system and V2V communication. This contributes to an accurate and effective real-time motion planning strategy in the system.
- We propose a prediction method to learn optimal motion planning of the participated AVs. This helps to understand how AVs and the perception system interact in the system framework.
- We validate the performance of the proposed system model with different case studies in autonomous driving simulator CARLA. We find that through the proposed system framework, the robustness of the perception system can be guaranteed with available V2V communication. Furthermore, the effectiveness of the lane-change motion planning strategy can also be achieved.

The rest of this paper is organized as follows. Section II examines closely related studies and identifies the challenges that motivate this work. SectionIII then develops the system model. In Section IV, the AV motion planning problem is formulated by incorporating the perception system. Next, SectionV details the case studies conducted to evaluate the proposed system model. Finally, Section VI concludes this work and provides possible future research directions.

II. Related Work

Several AV motion planning strategies have been proposed for reliable and safe maneuver operations [5]–[7], [29]. For instance, [5] proposed an efficient motion planning method for AV on-road driving through rapidly exploring random tree algorithm. A novel local motion planning hierarchical framework was conducted in [6] for AVs to track a reference trajectory and effectively avoid obstacles. In [7], a probabilistic method was built for real-time decision making and motion planning for AVs. In addition, [29] presented a novel coordination approach for motion planning of connected vehicles, especially intersection environment management. Upon the same environment, [8] developed a motion-planning model for urban autonomous driving at uncontrolled intersections of road networks. Considering highway traffic roads, [9] investigated the motion planning approaches with a focus on highway planning of AVs. Besides, lane-change motion is one of the essential component of lateral AV motions, which can affect the surrounding vehicles and further impact the traffic flow collectively. There are some existing studies focusing on planning AV lane-change motions. In [10], a back-to-back performance on different lane-change maneuvers was demonstrated, which included two automated driving approaches and manual driving. Considering dynamic vehicular constraints, a stochastic model-predictive control problem was formulated in [12] to keep the automated driving vehicle. In addition, [15] proposed a lane-change strategy considering other AVs' velocity prediction, motion planning, and trajectory tracking control. Furthermore, [13] proposed an autonomous lane-change decision-making model that implemented benefit, safety, and tolerance factors. However, these work neglect the consideration of dynamic traffic conditions, which may cause collisions due to occurrence of sudden accidents. The feasible maneuvers are timely associated with the time-varying traffic environment. Hence, in order to capture the time-varying dynamic traffic conditions, several existing studies investigated the effect of V2V communication on lane-change motion planning, e.g. [30], [31]. For instance, a lane change warning system was proposed in [30] to obtain the surrounding vehicle' motion states via V2V communication. By means of V2V communication techniques, [31] proposed a model

to consider the traffic scene with multiple mandatory lane change demands and completed the trajectory planning for vehicles by taking the safety and efficiency into consideration. Besides, the use of deep learning techniques contribute to the reliable and safe AV lane-change motion by learning optimal planning paths, since they can timely capture the real-time traffic conditions. Through a reinforcement learning technique, a cooperative lane-changing strategy in [11] was developed to enable lane-changing behavior in consideration of traffic efficiency. In [14], a comprehensive model that considered different time-to-lane naturalistic crossings based on a back propagation neural network was proposed, which was optimized by a particle swarm optimization algorithm. Although these researches implement deep learning techniques into AV lane-change motion strategies, they do not involve the utilization of perception systems installed at AVs.

By considering the utilization of perception systems, known as INVS, the AV lane-change motion planning strategy can be further optimized in a reliable manner. The perception systems are developed from the ground up to support the development, training, and validation of AV urban driving systems. There are some typical perception systems utilized for modeling the virtual traffic environment, including suggested upper merged ontology (SUMO) [32] and CARLA [33]. These systems are capable of supporting flexible specifications of sensor suites and environmental conditions in traffic networks. Several existing studies have implemented V2V communication techniques into the perception systems to further contribute to the improvement of the robustness of these systems, thus making AVs move safer on the road. For example, [26] comprehensively discussed the framework of cooperative V2V communication in the computation of the vehicular perception system. In [27], a unified cooperative perception framework was evaluated by employing V2V communication connectivity. Furthermore, [28] analyzed the necessary dynamic information for the cooperative perception to enable safe and reliable automated driving. However, these systems may be more concerned about the quality of map fusion, as well as the degradation issue of the sensing and model uncertainties. The robustness of the perception system is related to real-time AV motion planning, in order to maintain a reliable and safe lane-change motion. In this work, we consider evaluating the robustness of the CARLA system with V2V techniques. The evaluation considers the effects of the communication losses in the ad-hoc V2V network and the unpredictable vehicle motions in traffic by on-board sensors. Additionally, the future context information generated by the CARLA system can be used for learning the optimal motion planning of the ego AV.

III. System Model

This section illustrates the proposed system framework, as shown in Fig. 2. It contains four major components, known as environment, V2V communication, perception system, and operation of AVs. The proposed system possesses the following characteristics to enable the feasibility of the entire operations.

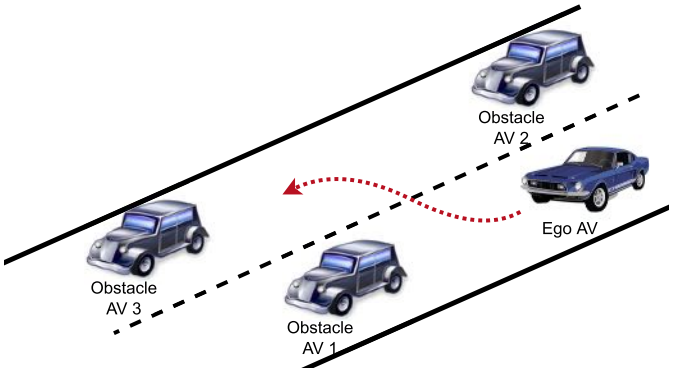

Fig. 1. A typical scenario of AV lane-change motion.

A. Environment

The physical-world implementation of autonomous driving is hindered by the infrastructure costs and the difficulties of testing in dangerous environment. Consequently, this paper adopts CARLA, a widely-accepted unreal-engine driven benchmark system, to provide complex urban driving scenarios and high 3D rendering quality, to model the environment. In this work, we model the road network to represent the AV lane-change motion scenario within a particular area shown in the specific block of Fig. 2. Consider a typical case depicted in Fig. 1, which includes four AVs moving on two straight lanes. The top lane is the target lane (TL) while the bottom one is the ego lane (EL). The ego AV is initiated on the EL. Besides the ego AV, there are three obstacle AVs moving on these two lanes. The lane width of this case follows the real-world road design standard listed in [34], which can be set to 3.7 meters. The entire period of lane-change motion for the ego AV is denoted as $\mathcal{T}$, which can be divided into N_T time steps. The interval of each time step is defined as Δt.

Besides, we denote the set of the obstacle AVs as $\mathcal{N}$ with different properties. These AVs are assumed to be stay at their lanes during the entire period of the lane-change motion. For the AV configurations, we denote l and w as the length and width of each AV, including both the ego AV and obstacle AV. In addition, h is defined as the wheeling length of each AV. The ego AV shall determine a suitable longitudinal acceleration and lateral yaw rate during the entire period, in order to meet the requirements of vehicle dynamics and obstacle avoidance. Moreover, the success of lane-change motion is guaranteed by the efficiency and safety of the movement of the ego AV, which considers small acceleration and jerk so that the safe distance between the ego AV and other obstacle AVs can be satisfied.

B. V2V Communication

The V2V communication module is the core of the entire system framework, which is responsible for the wireless communication among the ego AV, the obstacle AVs, and the perception system. The lane-change motion planning and scene parameters detected by the obstacles AVs can be delivered to the ego AV via the V2V communication module. In the meantime, the parameters can also be transmitted by this module, such as position, velocity, acceleration rate, and

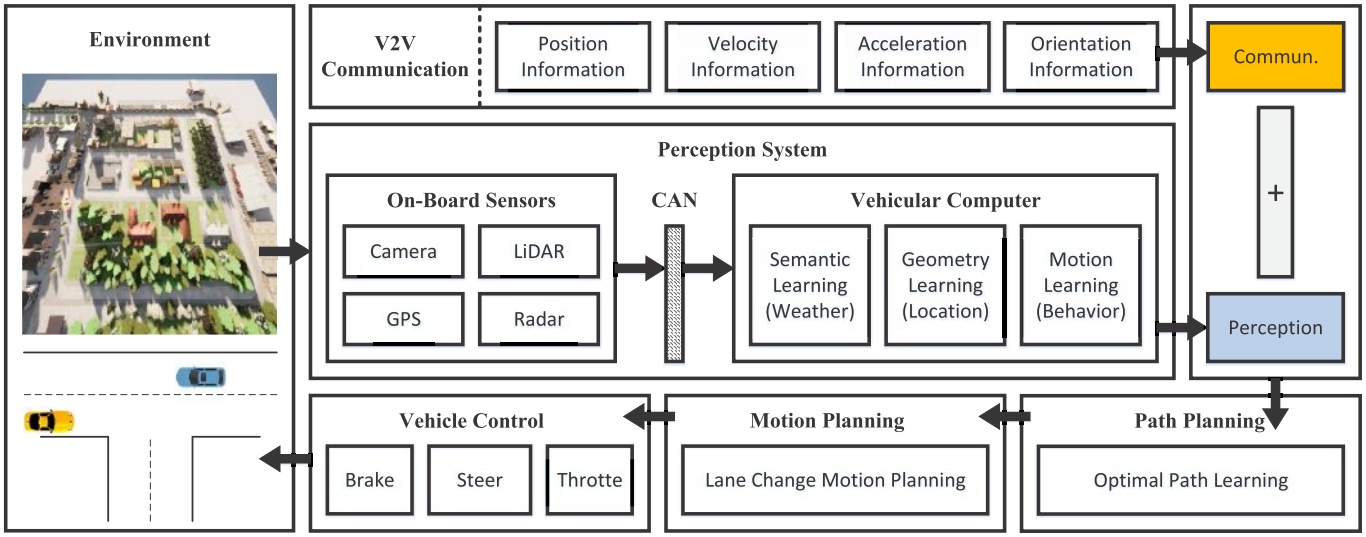

Fig. 2. The proposed system framework, which contains environment to generate road traffic, a V2V communication module to guarantee information transmission flows of vehicular features, a perception system to perform feature sensing and prediction, and autonomous vehicles to proceed motion learning, planning, and control.

orientation of all participated AVs, which are shown in the block of V2V communication module in Fig. 2. Otherwise, the occurrence of the random outage, latency, packet loss can lead to the unsuccessful V2V communication, which may further cause traffic crashes due to insufficient information received when performing lane-change motion. Furthermore, with the development of wireless communication, such as 6G technology, the vehicular network analysis, planning and optimization shall be raised from two dimensions to three dimensions so as to further improve the motion planning strategy of AVs [35]. Note that we follow the V2V communication range standard in [36].

C. Perception System

The perception system includes two main components, namely, on-board sensors and vehicular computer. The specific details of each components are listed below.

For the on-board sensors, light detection and ranging (LiDAR) is assumed to be installed at all participated AVs. LiDAR is an active near visible band sensor that can build up a three-dimensional map of the scene by measuring the time of flight of pulsed light. By using LiDAR, the surrounding scene of vehicle can be scanned. However, various weather conditions can affect the scanning process of the LiDAR. The lane-change motion may be affected by the bad weather conditions, such as rainy weather. The blurred images obtained by the perception system leads to imprecise detection of the distance range between the ego AV and the obstacle AVs. During the period of lane-change motion, we define a time-varying rain rate as $R(t)$, where $t = \{1, \ldots, N_T\}$. According to [37], the performance of LiDAR sensors can be affected by the rainy weather. Specifically, the modified distance is varied by the different level of rain rates. Hence, we can model such relationship as follow

$$d_{\text{modified}}(t) = d_{\text{detect}}(t) + \zeta d_{\text{detect}}(t)(1 - e^{-R(t)})^2 \quad (1)$$

where $R(t)$ refers to the rain rate at time t and ζ denotes the variance vector. $d_{\text{detect}}(t)$ presents the detected distance under normal conditions at time t. In this work, we set $\zeta = 0.02$, similar to the setting in [37]. In addition, the sizes of the raindrops are assumed to be the same.

Through the information transmitted via the clustering of applications (CAN), the vehicular computer is responsible for the context prediction. The function of context prediction is used to monitor and predict the real-time traffic conditions. In this function, data collection gathers the sensing data under different scenarios. When the data is collected, the data preprocessing is needed for the purpose of efficient model training by means of a novel deep learning approach. The model pretraining stage is able to output the initial model parameters. The number of samples for every individual scenario is determined by the learning curves shown in [38].

The vehicular computer is mainly responsible for data processing, including voxelization, convolution, regional proposal generation, regression, classification, and orientation. Also, the proper use of the deep learning can contribute to an accurate prediction on the conditions of traffic networks, such as traffic speed prediction [39]. These modules are utilized via the perception system to perform several operations, such as practical road simulation, weather simulation, data classification and analysis, and so on. Considering the aggregated vehicular information, the perception system then transmits the information to the ego AV and obstacle AVs through the broadcast signals via the Internet. Besides, these scene parameters can further help perform lane-change motion by real-time interaction between the ego AV and the perception system.

To combine with the V2V communication system, the communication-perception information fusion model is proposed, which is illustrated in Fig. 3. The output of this fusion model is the positions and velocities of ego and obstacle vehicles that will be subsequently used for collision avoidance motion planning. The input of this fusion model includes:

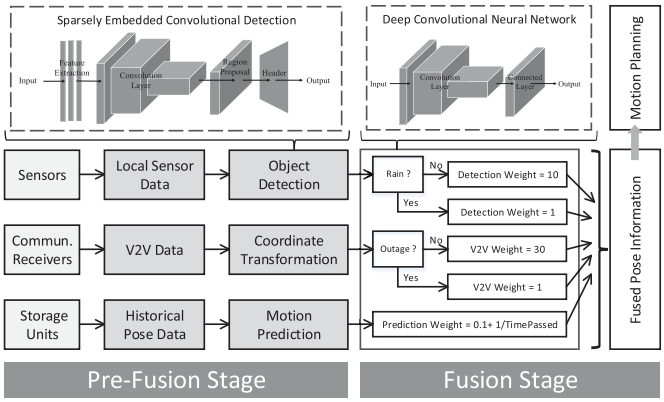

Fig. 3. Flowchart of system operation.

1) sensory data; 2) communication data; 3) historical data. These three types of data are processed in parallel, where the senor data is fed into a deep sparsely embedded convolution detection network for object detection, the received V2V data is transformed from global to local coordinate system, and the historical pose data is extrapolated to predict the current poses of obstacle vehicles. After the above processing pipeline, all types of data are transformed into poses in the same local coordinate system. They can be directly merged by performing the weighted sum. The weights of different data sources are computed as follows. For the object detection result, a deep convolutional neural network (CNN) is adopted to classify the current weather. The weight is set to 1 if raining and 10 otherwise. The V2V result is computed based on the dynamic map fusion technique in [21], which achieves higher map quality than ego-vehicle perception. Consequently, the weight is set to 30 if the V2V data is successfully received and 1 otherwise. Finally, the weight of poses obtained from motion prediction is set as inversely proportional to the duration between the current time and the data storage time.

D. Operation of Autonomous Vehicles

The operation of AVs in the system mainly involves three functions, namely, path planning, motion planning, and vehicle control. First of all, the operation is incurred in the information stage based on the behaviors of the status of the participated obstacle AVs. These AVs in the system have been installed with on-board sensors to capture the traffic information of the surrounding environment. Then, the ego AV mainly performs the three functions mentioned previously. At the planning stage, for path planning, it is related to motion learning by tackling sensing real-time uncertainties of the surrounding environment. This function helps the ego AV to learn the optimal path under different circumstances. In addition, motion planning function is associated with the strategy lane-change motion of the ego AV. After that, based on the planning strategy, at the control stage, the ego AV is controlled by operating the vehicle brake, steer, and throtte. The related parameters include the lateral position, velocity, acceleration rate, and yaw angle of the ego AV. Considering these four factors, we define them as $\mathcal{P}_{\text{ego}}$, v_{ego}, a_{ego}, and θ_{ego}, respectively, where $\mathcal{P}_{\text{ego}} = \{x_{\text{ego}}, y_{\text{ego}}\}$ to further illustrate the x-position and y-position of the ego AV.

TABLE I
TABLE OF PARAMETERS FOR PROPOSED SYSTEM

Parameters	
$\mathcal{T}$	Index set of time period
N_T	Total number of timeslot
δt	Timeslot
l	Length of AV
w	Width of AV
h	Wheeling length of AV
R_t	Rain rate
$d_{\text{detect}}(t)$	Detected distance at time t
$d_{\text{modified}}(t)$	Modified distance at time t
ζ	Variance vector
$\mathcal{P}_{\text{ego/obs}}$	2-D dimension vector of ego/obstacle AV
v_{obs}	Velocity of obstacle AV
a_{obs}	Acceleration of obstacle AV
θ_{obs}	Yaw angle of obstacle AV
ω_{obs}	Angular velocity of obstacle AV
$\mathbf{RO}$	Orthogonal rotation matrix
$\mathbf{t}_r$	Translation vector
μ	Road adhesion coefficient
g	Thickness of the water film
Δ^n_{safe}	Safe distance between ego AV and obstacle AV n
$x^n_{\text{obs,leader}}$	Longitudinal position of leader obstacle AV n
$v^n_{\text{obs,leader}}$	Velocity of leader obstacle AV n
$x^n_{\text{obs,follower}}$	Longitudinal position of follower obstacle AV n
$v^n_{\text{obs,follower}}$	Velocity of follower obstacle AV n
τ^n	Reaction time for obstacle AV n
d_{min}	Minimum distance to avoid collision
α^n	Maximum de-acceleration rate of obstacle AV n
$d^{\text{rec}}_{\text{min}}$	Minimum distance with V2V
$d^{\text{est}}_{\text{min}}$	Estimated minimum distance without V2V
$d^{\text{per}}_{\text{min}}$	Minimum distance with perception system
M_f	Maximum iteration number
ϵ_f	Convergence tolerance
Optimization variables	
v_{ego}	Velocity of ego AV
a_{ego}	Acceleration of ego AV
θ_{ego}	Yaw angle of ego AV
ω_{ego}	Angular velocity of ego AV

The above system framework inherently consists of two novel techniques:

- Lane-change motion planning by tackling obstacle avoidance while performing context prediction in real-time;
- Motion learning by tackling sensing uncertainties.

In the following sections, we will introduce these two approaches in a detailed manner.

IV. AUTONOMOUS VEHICLE LANE-CHANGE MOTION PLANNING

As discussed in Section III, the key problem is to investigate the optimal lane-change strategy for ego AV by means of effective scene perception and V2V communications. The problem formulation is shown as follows.

A. Operational Constraints

1) Autonomous Vehicle Dynamics: The AV dynamics are utilized to represent the vehicular motion on the road. Consider that the motion planning is taken place over a specific time period $[T_{start}, T_{end}]$, which can be discretized equally into N_T

time slots. The interval of every time slot is defined as Δ_t. Then, we define the state vector for the ego AV as

$$u_{\text{ego}} = \begin{bmatrix} x_{\text{ego}} & y_{\text{ego}} & v_{\text{ego}} & a_{\text{ego}} & \theta_{\text{ego}} \end{bmatrix}, \tag{2}$$

where $x_{\text{ego}}, y_{\text{ego}}, v_{\text{ego}}, a_{\text{ego}}, \theta_{\text{ego}}$ denotes x-position, y-position, velocity, acceleration, yaw angle for the ego AV.

Besides the ego AV, we denote a set of other AVs $n \in \mathcal{N}$ as obstacle AVs in the road system. The state vector for such AVs can be defined as

$$u^n_{\text{obs}} = \begin{bmatrix} x^n_{\text{obs}} & y^n_{\text{obs}} & v^n_{\text{obs}} & a^n_{\text{obs}} & \theta^n_{\text{obs}} \end{bmatrix}, \ \forall n \in \mathcal{N}, \tag{3}$$

where $x^n_{\text{obs}}, y^n_{\text{obs}}, v^n_{\text{obs}}, a^n_{\text{obs}}, \theta^n_{\text{obs}}$ denotes x-position, y-position, velocity, acceleration, yaw angle for the obstacle AV n.

To represent the inner relations of AV dynamics between the ego AV and obstacle AVs, the following constraints are developed

$$\begin{bmatrix} \frac{dx_{\text{ego}}}{dt} & \frac{dx^n_{\text{obs}}}{dt} \end{bmatrix} = \begin{bmatrix} v_{\text{ego}}\cos(\theta_{\text{ego}}), v^n_{\text{obs}}\cos(\theta^n_{\text{obs}}) \end{bmatrix}, \ \forall n \in \mathcal{N}, \tag{4}$$

$$\begin{bmatrix} \frac{dy_{\text{ego}}}{dt} & \frac{dy^n_{\text{obs}}}{dt} \end{bmatrix} = \begin{bmatrix} v_{\text{ego}}\sin(\theta_{\text{ego}}), v^n_{\text{obs}}\sin(\theta^n_{\text{obs}}) \end{bmatrix}, \ \forall n \in \mathcal{N}, \tag{5}$$

$$\begin{bmatrix} \frac{dv_{\text{ego}}}{dt} & \frac{dv^n_{\text{obs}}}{dt} \end{bmatrix} = \begin{bmatrix} a_{\text{ego}}, a^n_{\text{obs}} \end{bmatrix}, \ \forall n \in \mathcal{N}, \tag{6}$$

$$\begin{bmatrix} \frac{d\theta_{\text{ego}}}{dt} & \frac{d\theta^n_{\text{obs}}}{dt} \end{bmatrix} = \begin{bmatrix} \omega_{\text{ego}}, \omega^n_{\text{obs}} \end{bmatrix}, \ \forall n \in \mathcal{N}. \tag{7}$$

In addition, the above parameters in (4) - (7) follow the lower and upper limits in performing lane-change motion, respectively, which are shown as

$$\begin{bmatrix} v^{\text{ego}}_{\min}, v^n_{\min} \end{bmatrix} \le \begin{bmatrix} v_{\text{ego}}, v^n_{\text{obs}} \end{bmatrix} \le \begin{bmatrix} v^{\text{ego}}_{\max}, v^n_{\max} \end{bmatrix}, \ \forall n \in \mathcal{N}, \tag{8}$$

$$\begin{bmatrix} a^{\text{ego}}_{\min}, a^n_{\min} \end{bmatrix} \le \begin{bmatrix} a_{\text{ego}}, a^n_{\text{obs}} \end{bmatrix} \le \begin{bmatrix} a^{\text{ego}}_{\max}, a^n_{\max} \end{bmatrix}, \ \forall n \in \mathcal{N}, \tag{9}$$

$$\begin{bmatrix} \omega^{\text{ego}}_{\min}, \omega^n_{\min} \end{bmatrix} \le \begin{bmatrix} \omega_{\text{ego}}, \omega^n_{\text{obs}} \end{bmatrix} \le \begin{bmatrix} \omega^{\text{ego}}_{\max}, \omega^n_{\max} \end{bmatrix}, \ \forall n \in \mathcal{N}. \tag{10}$$

Furthermore, we define **RO** as an orthogonal rotation matrix and $\mathbf{t}_r$ as a translation vector. This matrix is a function of the vehicle moving angle $\theta(t)$ at time step t. The translation vector $\mathbf{t}_r(\cdot)$ is a function of the longitudinal $x_{\text{ego}}(t)$ and lateral $y_{\text{ego}}(t)$ positions of the ego AV. Hence, the transformed polytope can be represented with the x and y coordinates in two dimensional space. The matrix $\mathbf{A}$ and the vector $\mathbf{b}$ are defined as

$$\mathbf{A} = \begin{bmatrix} \mathbf{RO}(\theta(t))^T \\ -\mathbf{RO}(\theta(t))^T \end{bmatrix}, \ \forall t \in \mathcal{T}, \tag{11}$$

$$\mathbf{b} = \begin{bmatrix} \frac{l}{2}, \frac{w}{2}, \frac{l}{2}, \frac{w}{2} \end{bmatrix}^T + \mathbf{A}\begin{bmatrix} x_{ego}(t), y_{ego}(t) \end{bmatrix}^T, \quad \forall t \in \mathcal{T}, \tag{12}$$

where $(\cdot)^T$ means the transpose of the matrix. l and w denote the length and width of the ego AV, respectively. The rotation matrix of the ego AV at each time step t is computed by

$$\mathbf{RO} = \begin{bmatrix} cos(\theta(t)) & -sin(\theta(t)) \\ sin(\theta(t)) & cos(\theta(t)) \end{bmatrix}, \quad \forall t \in \mathcal{T}. \tag{13}$$

The occupied area for each AV in the system is modeled as a time-varying polytope. At each time step, the motion planning is performed to ensure that there is no intersection occurs between the polytopic sets.

Considering different weather conditions, the road adhesion characteristic is needed to be tackle when formulating the vehicle dynamics. We follows the similar formulations of vehicle dynamics under the severe weather shown in [40]. In this reference, for rainy weather, the road adhesion coefficient is related to vehicle states, e.g. vehicle speed, and it is calculated via the equation $\mu = 0.9458 - 0.0057 v_{\text{ego}} - 0.0108 g$, where g is the thickness of the water film. Since severe weather conditions have a huge impact on the adhesion coefficient of the road and the vehicle tyres, the tyre saturated lateral force cannot supply the vehicle steering centrifugal force. Hence, the case of sideslip is more likely to occur while steering on a highway. In this case, the vehicle acceleration threshold in rainy conditions shall be lower, and it can be calculated as:

$$a_{\text{ego, max}} = \mu g. \tag{14}$$

The typical situation is a sharp turn when vehicle sideslip occurs, and this example is shown as Fig. 2 in [40]. In the meantime, the variables of the ego AV, such as vehicle speed, lateral/longitudinal acceleration, yaw angle, and angular velocity, are substantially affected.

2) Obstacle Avoidance: As mentioned in Section III, the purpose of the ego AV is to travel in an efficient way through the lane-change motion planning strategy. To enable a safe lane-change motion of the ego AV, we define a safe distance between the ego AV and the obstacle AV n, which is denoted as Δ^n_{safe}. During the process of lane-change motion, we assume that when the ego AV is in the ego lane, it should keep the safe distance between the ego AV and the leader obstacle AV initially. In addition, when the ego AV traverses to the target lane, the ego AV should avoid the potential collisions between the leader and follower obstacle AV n so as to keep the safe distance. Hence, the constraint related to the safety distance is denoted as

$$\Delta^n_{\text{safe}} \le \begin{cases} x^n_{\text{obs,leader}} - x_{\text{ego}} & \text{if ego AV at the ego lane,} \\ x^n_{\text{obs,leader}} - x_{\text{ego}} & \text{if ego AV at the target lane,} \\ x_{\text{ego}} - x^n_{\text{obs,follower}} & \text{if ego AV at the target lane,} \end{cases} \tag{15}$$

where $x^n_{\text{obs,leader}}$ and $x^n_{\text{obs,follower}}$ represent the longitudinal position of the leader and follower obstacle AV n, respectively. Besides, according to [41], we implement the critical warning distance between each pair of AVs, which consists of the reaction time and de-acceleration rate when the sudden accident occurs. Hence, we merge the concept of the critical distance to the safe distance between the ego AV and the obstacle AV $n \in \mathcal{N}$, and it can be calculated by

$$\begin{aligned} \Delta^n_{\text{safe}} &= f(v^n_{\text{obs,leader}}, v^n_{\text{obs,follower}}) \\ &= \frac{1}{2}\left(\frac{(v^n_{\text{obs,follower}})^2}{\alpha^n} - \frac{(v^n_{\text{obs,leader}})^2}{\alpha^n}\right) \\ &\quad - v^n_{\text{obs,follower}}\tau^n + g^n(\beta, d_{\min}), \end{aligned} \tag{16}$$

where τ^n denotes the reaction time for the obstacle AV n and d_{min} represents the minimum distance required to avoid collisions until both vehicles have full stops. Moreover, α^n is

defined as the maximum de-acceleration rate of the obstacle AV n. Note that, to consider the bad weather condition, d_{min} can be replaced by d_{detect} shown in (1). Then, the function $g^n(\cdot)$ denotes the availability of V2V communication in obstacle AV n, which is given by

$$g^n(\beta(t), d_{\min}) = (1-\beta(t))d_{\min}^{\text{rec}} + \beta(t)d_{\min}^{\text{est}}, \tag{17}$$

where $\beta(t)$ represents the binary parameter of the availability of V2V communication at time t within the process of lane-change motion. Moreover, $d_{\min}^{\text{rec}}$ represents the minimum distance if the ego vehicle has received V2V information, while $d_{\min}^{\text{est}}$ denotes the estimated minimum distance if the V2V communication fails, where the object information is obtained from deep learning perception or calculated with the estimated velocity and acceleration rate. Note that these two values are not equal, and they satisfy the condition of $d_{\min}^{\text{rec}} \leq d_{\min}^{\text{est}}$, which requires much safer distance since the estimated result may not accurate if the sudden accident occurs.

Furthermore, during the procedure of lane-change motion, the ego AV can timely interact with the perception system to adjust the motion planning strategy. Meanwhile, the safety distance between the ego AV and the obstacle AVs can be detected via the perception system in real-time. We denote $d_{\min}^{\text{per}}$ as the minimum distance if the ego vehicle has received the value from the perception system. Then, we define the binary parameter u to indicate the connectivity between the AV and the perception system. The following equation indicates the availability of the perception system

$$d_{\min}^{\text{per}} = \begin{cases} d_{\text{detect}} & \text{if } u = 1, \\ \max(d_{\min}^{\text{rec}}, d_{\min}^{\text{est}}) & \text{if } u = 0, \end{cases} \tag{18}$$

where $\max(\cdot)$ denotes the maximum operation of these values. In addition, the second condition in (21) holds when the V2V communication succeeds.

Furthermore, we can use the measurements at time step k to estimate the future status of each AV. Without the future information from V2V communication and CARLA perception system, the future values of the obstacle AVs can be estimated by using the following two equations:

$$v_{\text{obs}}^{n,\text{est}}(k+1|t) = v_{\text{obs}}^{n}(k|t) + a_{\text{obs}}^{n}(k|t)\Delta t. \tag{19}$$

Besides, the estimated moving distance of the obstacle AV n can be calculated by

$$x_{\text{obs}}^{n,\text{est}}(k+1|t) = x_{\text{obs}}^{n}(k|t) + v_{\text{obs}}^{n}(k|t) + \frac{1}{2}a_{\text{obs}}^{n}(k|t)(\Delta t)^2. \tag{20}$$

B. Vehicle-to-Vehicle Communication

The proposed system framework assumes that each AV is equipped with senors for V2V communication. The ego AV in the road system is capable of receiving the transmitted information from other obstacle AVs when proceeding the lane-change motion. The forecast information is corresponding to the future velocity trajectory of these obstacles AVs, which can be given by the CARLA system. The mathematical representation of the forecast information of the obstacle AV $n \in \mathcal{N}$ can be denoted as

$$v_{\text{obs,leader}}^{n,\text{forecast}} = \left[v_{\text{obs,leader}}^{n}(t|t); \ldots; v_{\text{obs,leader}}^{n}(t+N_T|t)\right], \tag{21}$$

$$v_{\text{obs,follower}}^{n,\text{forecast}} = \left[v_{\text{obs,follower}}^{n}(t|t); \ldots; v_{\text{obs,follower}}^{n}(t+N_T|t)\right]. \tag{22}$$

For the above representation, $v_{\text{obs,leader}}^{n}(k|t)$ and $v_{\text{obs,follower}}^{n}(k|t)$ are the planned velocities for the obstacle leader/follower AV n at each time step k. When the ego AV receives the forecast velocities of the leader and follower obstacle AVs, this information can be used for distance tracking so as to keep the safe distance between the ego AV and each obstacle AV. Besides the forecast velocity, each AV is able to transmit its own current radar measurement, GPS coordinates, acceleration rate, and perception images of the surrounding scene. As mentioned in Section III, each AV checks the current status of motion through the information received through V2V communication. Moreover, when each AV receives the incoming message, it is capable of verifying the ID of the surrounding AVs and indicating their current positions.

C. Deep Learning Perception

If V2V communication fails, then the objects are detected by perception models or by estimation. In our system, the perception models need to extract two types of information from the raw data: 1) the semantic information such as weather, road, and traffic conditions, which helps to judge the scene complexity and determine the driving mode (aggressive or conservative); 2) the geometry information such as the location, length, width, and height of objects, which is necessary for motion planning and obstacle avoidance.

For the first perception task, we use the camera images as the input data, and train a 6-layer CNN for weather classification. In particular, the input image is sequentially fed into a 5×5 convolution layer (with ReLu activation, 32 channels, and SAME padding), a 2×2 max pooling layer, then another 5×5 convolution layer (with ReLu activation, 64 channels, and SAME padding), a 2×2 max pooling layer, a fully connected layer with 128 units (with ReLu activation), and a final softmax output layer (with 2 outputs representing raining or not).

For the second perception task, we use the LiDAR point clouds ad the input data, and train a sparsely embedded convolutional detection (SECOND) neural network for object detection. In particular, the SECOND net is a voxel-based neural network that converts a point cloud to voxel features, and sequentially feeds the voxels into two feature encoding layers, one linear layer, one sparse CNN and one RPN. The training dataset for SECOND should consist of four parts: 1) color and gray scale images captured by the high-resolution camera, 2) geographic coordinates including altitude, global orientation, velocities, accelerations, angular rates, accuracies and satellite information, 3) point cloud data from the LiDAR, and 4) object labels in the form of 3D tracklets.

D. MPC-Based Lane-Change Motion Planning

The proposed MPC-based lane-change motion planning problem use a receding horizon fashion. The optimization problem is solved and the control state vector is obtained at each time step. For the next time step, the time horizon is shifted forward and the process is repeated until the time ended. The objective function penalizes the deviation between the reference trajectory and the real trajectory generated by the problem, which is given by

$$\begin{aligned}&\Phi(\{x_{\text{ego}}(k), y_{\text{ego}}(k), a_{\text{ego}}(k), \omega_{\text{ego}}(k)\}_{k=1}^{N_T})\\&= \sum_{k=0}^{N_T} \left(x_{\text{ego}}(k) - x_{\text{ego}}^{\text{ref}}, y_{\text{ego}}(k) - y_{\text{ego}}^{\text{ref}}\right)^T\\&\quad \cdot \mathbf{Q}(x_{\text{ego}}(k) - x_{\text{ego}}^{\text{ref}}, y_{\text{ego}}(k) - y_{\text{ego}}^{\text{ref}})\\&\quad + \sum_{k=0}^{N_T-1} (a_{\text{ego}}(k) - a_{\text{ego}}(k-1), \omega_{\text{ego}}(k) - \omega_{\text{ego}}(k-1))^T\\&\quad \cdot \mathbf{W}(a_{\text{ego}}(k) - a_{\text{ego}}(k-1), \omega_{\text{ego}}(k) - \omega_{\text{ego}}(k-1)), \quad (23)\end{aligned}$$

where $x_{\text{ego}}^{\text{ref}}$ and $y_{\text{ego}}^{\text{ref}}$ denote the x- and y- direction reference trajectory, respectively, and $\mathbf{Q}$ and $\mathbf{W}$ are positive semidefinite weighting matrices. On the other hand, the obstacle avoidance constraints are implemented to guarantee the safe distance between the ego AV and each obstacle AV. Hence, the optimization problem is formulated as

$$\begin{aligned}&\textbf{minimize } \Phi(\{x_{\text{ego}}(k), y_{\text{ego}}(k), a_{\text{ego}}(k), \omega_{\text{ego}}(k)\}_{k=1}^{N_T}) \quad (24a)\\&\textbf{subject to } (8)-(10) \text{ and } (15) \quad (24b)\end{aligned}$$

In order to solve this problem in an efficient manner, we devise a related algorithm, shown in Algorithm 1. The time complexity of the formulated problem is $\mathcal{O}(1)$ at every time step. For every iteration m at time step k, the optimization problem is solved so as to obtain the solution, $[x_{ego}^m(k), y_{ego}^m(k)]$. Once the convergence conditions are satisfied, the optimal solutions are gained. Otherwise, the latest result is utilized as the initialization for the next iteration. We define that the iteration number is set as $m = M_f$, where M_f is the maximum iteration number. Lastly, the convergence tolerance is defined as $\epsilon_f = 10^{-5}$.

E. Learning Optimal Lane-Change Motion Planning

Based on the proposed lane-change problem formulated previously, it can be solved with certain iterations to obtain the optimal solution through Algorithm 1. However, this method is restricted by its relatively long computation time so that it cannot be used in real-time. To tackle this issue, we propose an efficient approach to incorporate a novel deep learning method with the optimization problem. The motion trajectories obtained by solving the problem shall be diverse, which consists of both feasible and infeasible paths that may not follow the city traffic rules. In addition, it is not promising to directly learn the policy gained from the demonstration data. Hence, we deploy data-driven methods on the AVs, such as CNN [42], to help determine the actions on performing lane-change while following the city traffic rules. The reason is that CNN can handle spatial features of the vehicular information, e.g. lateral positions of participated AVs and surrounding scenes captured by the installed sensors. By using CARLA system under successful V2V communications, such vehicular information of the obstacle AVs can be received by the ego AV to help determine the better lane-change actions. As described in Section III, the perception learning results obtained by CARLA system can be represented by $v_{\text{obs,leader}}^{n,\text{rec}}$ and $v_{\text{obs,follower}}^{n,\text{rec}}$.

In this part, we divide the lane-change learning procedure into the following two stages. The first stage, known as the classification stage, is utilized to predict the road conditions that satisfy the traffic rules. If it does not meet the criterion, re-initialization is required. The second stage refers to the action generation stage. If the lane-change action is output from the first stage, the second stage shall activate and generate the specific instructions for the lane-change motion. Additionally, during the process of lane-change motion, collision detection is continuously activated. If a possible sudden collision occurs, the ego AV detects it and stops the process of lane-change motion. The complete lane-change motion learning procedure is shown in Algorithm 2.

Algorithm 1 Lane-Change Motion Algorithm

Initialize the status of the ego AV and the obstacle AVs $n \in \mathcal{N}$.
for $k = 1{:}N_T$ **do**
  for $m = 1{:}M_f$ **do**
    Solve the problem (16) and obtain the result $[x_{ego}^m(k), y_{ego}^m(k)]$.
    if the convergence conditions are satisfied **then**
      Update the optimal solutions as $[x_{ego}^m(k), y_{ego}^m(k)]$
    else
      Return to Step 3 in the **for** loop for another iteration.
      Set $k = k + 1$.
    end if
  end for
  Return $[x_{ego}^m(k), y_{ego}^m(k)]$ as $[x_{ego}^*(k), y_{ego}^*(k)]$.
end for

Algorithm 2 Lane-Change Learning Procedure

Initialize the states and motion task.
Classify the motion task.
if Initial states of AVs follow traffic rules **then**
  for $k = 1{:}N_T$ **do**
    Use the result output by the proposed system.
    if Check sudden collision and surrounding environment **then**
      Perform actions on obstacle avoidance.
    else
      Take over by the system.
    end if
  end for
else
  Return to Step 1 for re-initialization.
end if

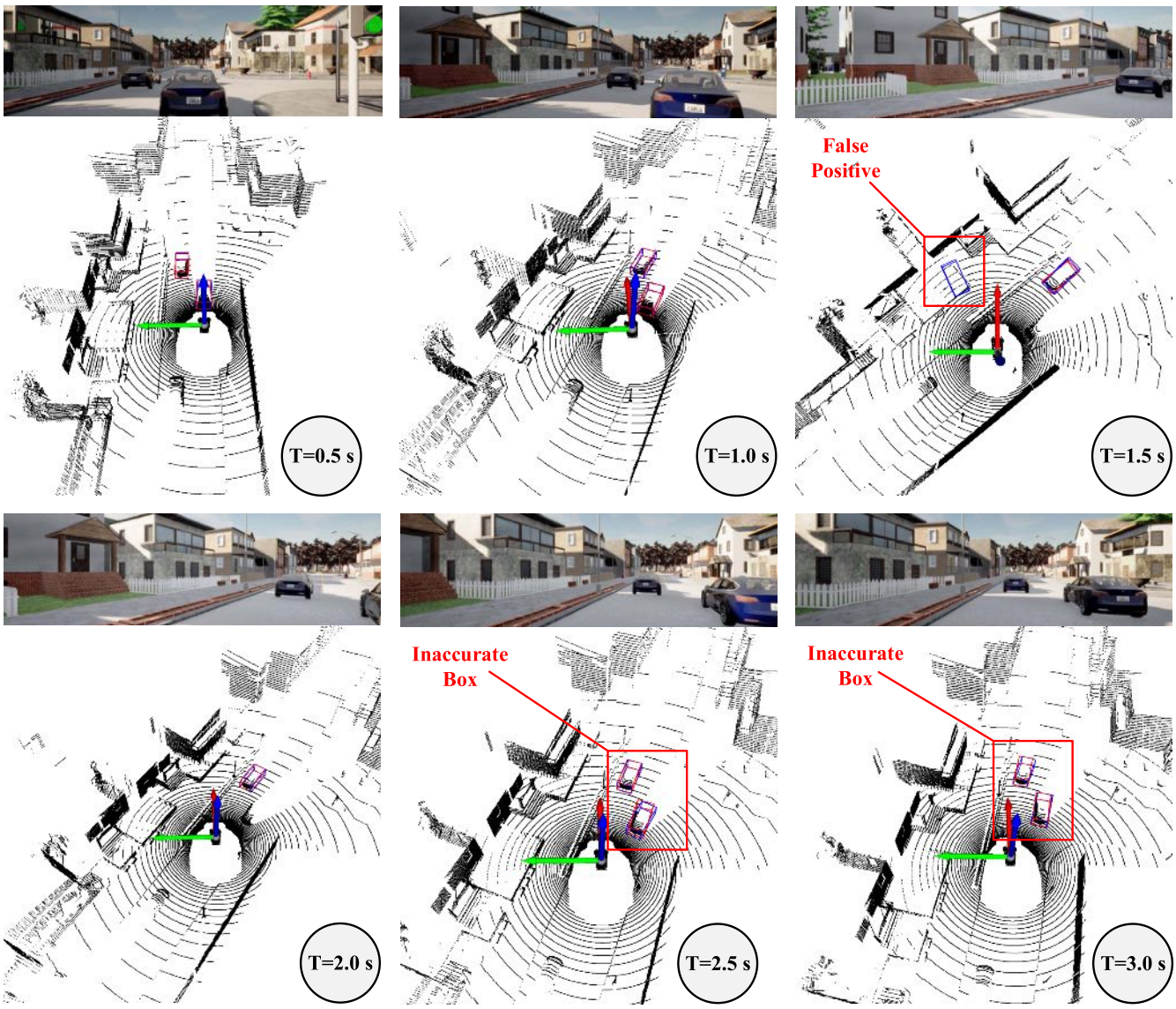

Fig. 4. Performance of the perception system during the lane-change motion.

V. Case Studies

In this section, we assess the performance of the proposed model. First, we detail our experimental setup. Then, we evaluate the proposed model in comparison of baseline techniques. Next, we compare three characteristic cases by using the proposed model. After that, we investigate the impact of different weather conditions and their effect on our proposed system model. Finally, we examine the robustness of the perception system and the convergence trend of the devised algorithm.

A. Simulation Setup

To demonstrate the real-world applicability of the proposed system model, we evaluate its performance in real-world systems. Specifically, our simulations are mainly conducted via the unreal engine platform generated by the CARLA system. The number of the total time period is set to 100 with Δt equals 0.05 seconds. During this time period, the rain rate $R(\mathcal{T})$ is generated via the CARLA system.

To train the CNN network for weather classification, we employ CARLA to generate 9 vehicles in the "Town02" map under both rainy and sunny weathers, among which 2 are autonomous driving vehicles that can generate the camera image data at a frequency of 10 frames/s. The entire dataset consists of 300 frames for training at each vehicle. To train the SECOND network, we employ CARLA to generate 28 vehicles in the "Town02" map, among which 4 are autonomous driving vehicles that can generate the point cloud data at a frequency of 10 frames/s. The entire dataset consists of 2800 frames in total with 700 frames at each vehicle, where 200 frames are used for training at each vehicle and 500 frames are used for validation. The Adam optimizer is adopted with a learning rate between 10^{-4} and 10^{-6}. The model training is implemented by PyTorch using python 3.8 on a Linux server with a NVIDIA RTX 3090 GPU.

Besides, our parameter settings for AV lane-change motion planning strategy are as follows. The road length is set to 7.4 meters with two separate lanes, which follows the standard

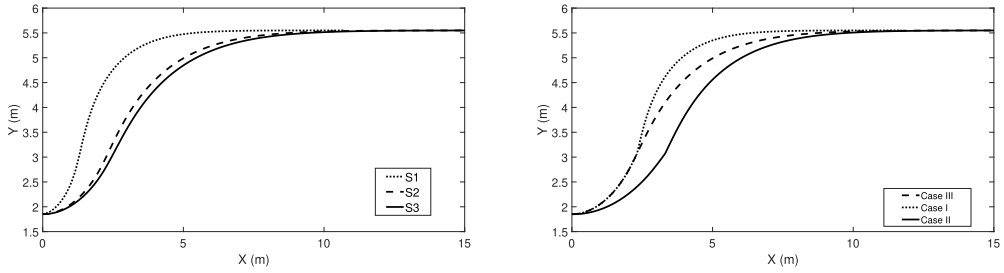

(a) (b)

Fig. 5. (a) Lane-change motion planning under different approaches. (b) Impact of lane-change motion planning under different cases.

in [34]. We consider that there are three obstacle AVs and one ego AV moving on these lanes. The initial locations of these AVs are set based on the positional data generated by the CARLA system. For each AV, the length is set to 4.7 meters while the width is set to 2.09 meters, which follows the specifications of Tesla Model 3 in [43]. The minimum safety distance d_{detect} between the ego AV and one obstacle AV is set to around 1 meter. According to the average latency of practical cellular systems [44], the one-way communication delay is assumed to be 100 milliseconds. The simulations are conducted using MATLAB Release 2017a with the `mosek` optimization solver found in the `yalmip` toolbox.

B. Effectiveness of Proposed System Model

First of all, this simulation studies the effectiveness of the proposed system model on the real traffic network. To measure the efficacy of the AV lane-change motion planning strategy provided by the proposed system, we compare the proposed model with the three baselines: 1) MPC approach in [45] without obstacle avoidance (S1); 2) proposed lane-change without the perception system (S2); 3) proposed lane-change with the perception system (S3).

Based on the configuration in Section V-A, we study the lane-change motion trajectories generated by the three baselines. In this part, we consider there are one ego AV and three obstacle AVs moving on the road. The result is presented in Fig. 5a. It is apparent that the trajectory generated in S2 outperforms S1. The reason is that, without the obstacle avoidance constraints, when the ego AV passes the intersection line, the trajectory is close to the location of the follower obstacle AV at the target lane. In the meantime, the safety distance of the ego AV and this obstacle AV cannot be guaranteed. Furthermore, since S2 can generate effective trajectory with the constraints of obstacle avoidance, it cannot suddenly change during the process of the lane-change motion. This is because S2 only considers that the movement of the three obstacles AVs follows the traditional motion equations in (19) and (20), which neglects the consideration of the perception system. By interacting with the perception, S3 can obtain the best lane-change trajectory since the proposed system model enables the timely interaction between the ego AV and the perception system, which can also be regarded as the difference between motion planning and path planning trajectories. Apparently, owing to the real-time interaction between the ego AV and the perception system, the AV lane-change motion planning strategy can be further improved in an efficient manner.

C. Impact of Different Cases

In this part, we investigate the lane-change motion planning trajectories under three following cases through the proposed model,

1) Case I: only one leader obstacle AV moving at the ego lane;
2) Case II: Case I + one leader and one follower obstacle AV moving at the target lane;
3) Case III: Case I + Case II;

Based on the traffic environment illustrated above, Case I only involves one obstacle AV at the ego lane while there is no AV at the target lane. Moreover, Case II considers the movement of two obstacle AVs at the target lane and there is only the ego vehicle traveling over the ego lane. Case III basically involves one ego AV and three obstacle AVs. Here we utilize the setting of S3 shown in the previous section so as to guarantee the availability of both V2V communication and perception system. The results of the AV lane-change motion trajectories are presented in Fig. 5b. In this figure, we can see that the proposed model performs effectively under these three cases. For instance, the curve (Case I) in Fig. 5b clearly indicates a sharp trajectory due to keeping the safety distance between the ego AV and the leader obstacle AV moving at the ego lane. Similarly, the curve (Case II) represents the trajectory to keep the safety distance when the ego AV moving at the target lane. Furthermore, the trajectory shown in this figure indicates the effective performance of Algorithm 2 since it is devised to perform the actions of obstacle avoidance for the ego AV.

In addition, by focusing on Case III, we further analyze the velocity and yaw acceleration rate profiles of the ego AV. The results are presented in Figs. 6a and 6b. In Fig. 6a, it is apparent that from the beginning of the time period, the ego AV increases the velocity for the lane-change motion. When it traverses on the target lane, the velocity keeps in a constant value. Besides, the yaw acceleration rate is relatively large when the ego AV performs the lane-change motion as shown in Fig. 6b. Additionally, at the target lane, the ego AV changes its acceleration rate in order to maintain a safe distance between the ego AV and the other two obstacle AVs. Last but not least, the profile of yaw angle is obtained as Fig. 6c, which further

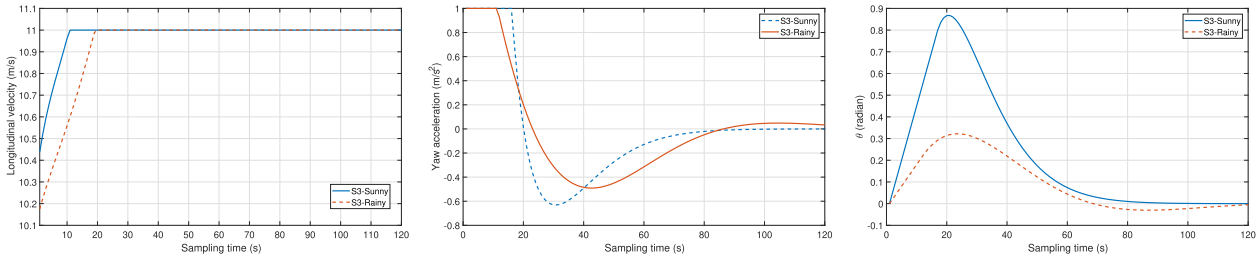

(a) (b) (c)

Fig. 6. (a) Profile of velocity from the ego AV. (b) Profile of yaw acceleration rate from the ego AV. (c) Profile of yaw angle from the ego AV.

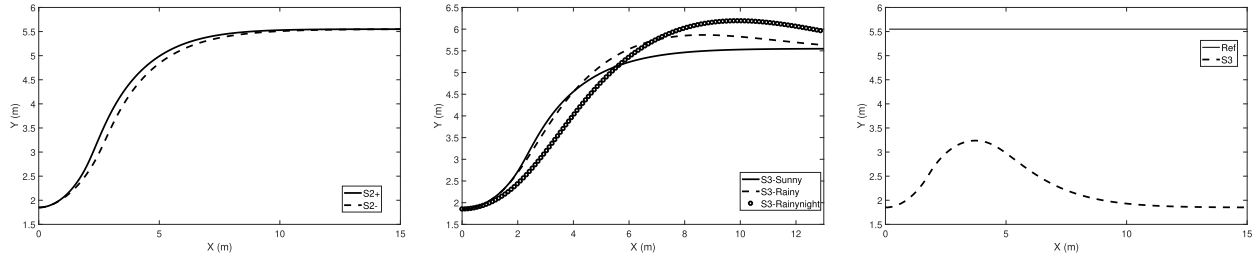

(a) (b) (c)

Fig. 7. (a) Effect of V2V communication reliability on lane-change motion planning. (b) Motion planning under different weather conditions. (c) Effect of proposed lane-change motion planning considering crossroads.

demonstrates the angle changes during the procedure of the lane-change motion from the ego AV.

D. Robustness of V2V Communication

Based on the setting of S2, we further assess the reliability and robustness of the V2V communication module. Since S2 denotes proposed lane-change without the perception system, we define S2+ as the one with the availability of V2V communication module while S2- is the one with the failure of V2V communication. Specifically, for the scenario S2-, the ego AV can only follow (19) and (20) to estimate the status of surrounding obstacle AVs. Meanwhile, we implement the Gaussian noise for indicating the errors of the received information via the V2V communication module. The result is presented in Fig. 7a. It is obvious that the trajectory of the ego AV (S2-) deviates as the errors occurred in V2V communication. Hence, by comparing the performance of S2+ and S2-, the reliability and robustness of the V2V communication module contribute to the stable trajectory of AV lane-change motion planning strategy.

E. Robustness of Perception System

We further investigate the robustness of the perception system that is incorporated in the proposed system framework. In this part, we validate the performance evaluation of Case III in the CARLA system. The results are shown in Fig. 4 and 8. In Fig. 4, for each subfigure, the top one indicates the visual image captured by the ego AV while the bottom one represents the sensing diagram of the radar. In particular, the sensing diagram can sense the surrounding scene of the ego AV in a multi-dimensional way. Since the interaction between the perception system and AV lane-change motion planning is operated in real-time, we capture eight screenshots of the perception results for every 0.5 second until $T = 4s$ as

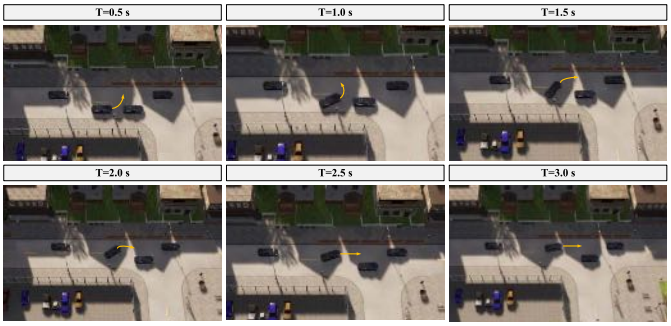

Fig. 8. Global lane-change motion planning under CARLA.

shown in Fig. 4. Each subfigure shows the crucial moment of the AV lane-change motion planning and the simultaneous visual images of the status of the ego AV. Besides, in Fig. 8, these eight instantaneous moments of the AV lane-change motion are captured via the CARLA system, which shows the consistency of the lane-change motion occurred in the results of Fig. 4. The complete trajectory is referred to the result of S3. Hence, these results demonstrate the robustness of the perception system utilized in the proposed system model.

F. Scene Perception Under Different Weather Conditions

In this part, we study the proposed model under different weather conditions during the total time period. In particular, as shown in Fig. 9, we have implemented four weathers: sunny day, rainy day, sunny night, and rainy night. Through the use of CNN, we are capable of simulating the practical weather conditions during the period of the AV lane-change motion. Specifically, the CNN model is trained on a dataset with 4000 different images and tested on a dataset with 1000 samples. Hence, the weather classification accuracy can reach 97%. Since the trained CNN can always distinguish sunny and rainy days, it may fail in classifying sunny and

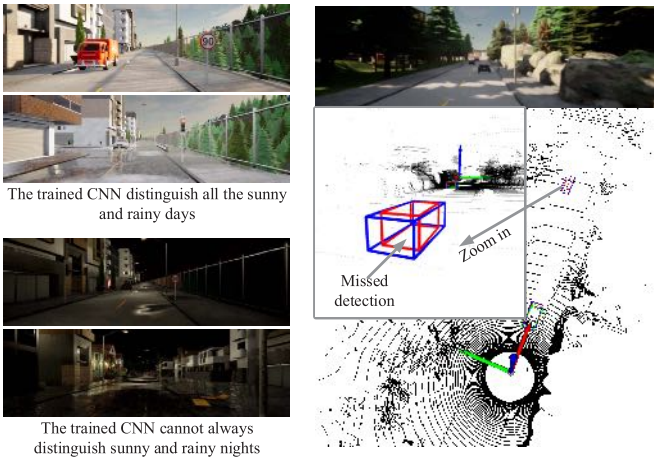

Fig. 9. Scene perception under different weather conditions.

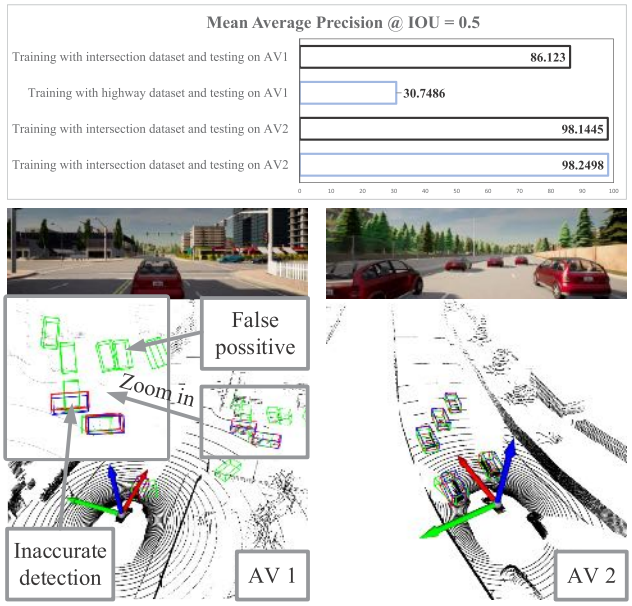

Fig. 10. Mean average precision performance at intersection and highway.

rainy nights. On the other hand, the right hand side sub-figure of Fig. 9 compares the pose information obtained from the ego-perception (green box), the V2V communication (blue box), and the ground truth (red box). It can be seen that the ego-vehicle fails in detecting one far-away object. However, its front vehicle can successfully detect the far-away object. This demonstrates that the V2V result is more accurate than the ego-vehicle result.

To correspond with these test environments, we further investigate the motion planning strategy under different weather conditions. Based on the setting in S3, we denote "S3-Rainy" as the motion planning trajectory under light rain condition while "S3-Rainynight" is the motion planning trajectory under heavy rain weather with extreme sliproad road condition. Here we follow [46], [47] to consider the success probability of safe driving under different sliproad conditions of rainy weather. In Fig. 7b, we can observe that the trajectories under rainy and rainy-night weather conditions include several deviations to the trajectory under sunny weather condition. The reason is that these two rainy weather conditions cause the occurrence of slippery road in different levels, which further affect the AV lane-change trajectory. Owing to the effectiveness of the perception system, the ego AV can immediately follow the target lane under the sliproad condition. Besides, compared to the profiles in Figs. 6a, 6b, and 6c, it indicates the changes of these vehicle states due to the effect of the rainy weather condition. These results are captured to demonstrate the effectiveness of scene perception of the proposed system model, which further improves the AV lane-change motion planning strategy under different weather conditions.

G. Impact of Different Road Conditions

Based on the setting of S3 under Case III, we further assess the effect of the proposed lane-change motion planning strategy when considering another road condition, e.g. the occurrence of crossroads. In practice, the traffic rule indicates that, before a vehicle enter the zone of crossroads, it must stay on its own lane without performing the lane-change motion within a certain distance. Hence, we consider such road condition to investigate the performance of the propose model. The result is shown in Fig. 7c. The solid line indicates the reference target lane for AV lane-change motion planning while the dashed line presents the actual lane-change motion trajectory for the ego AV. Apparently, the ego AV can follow the traffic rule since it does not fully cross the target lane and move back to the ego lane to enter the zone of crossroads. This result demonstrates the effectiveness of our proposed AV lane-change motion strategy under different road conditions.

Besides, we provide the average precision performance at two scenarios in the CARLA simulator, i.e., intersection and highway. Note that, for each scenario, we consider that four AVs are created and each vehicle collects 1000 point cloud frames. We use the first 500 samples for training and the rest for testing. The result is shown in Fig. 10. First, it can be seen that the model trained with the highway dataset breaks down in the intersection scenario, since the examples at the intersection are much more diverse than those at the highway. Second, the average precision of the model trained with the intersection dataset achieves 98% for the highway scenario and 86% for the intersection. This indicates that the trained model in one scenario can generalize to other scenarios.

H. Convergence of Devised Algorithm

This test evaluates the convergence of the devised algorithm shown in Algorithm 1. We study the proposed model under Case III. In the meantime, we consider the objective value of the optimization problem formulated in (20) and the corresponding convergence gap that is computed via the devised algorithm. In addition, the convergence gap is related to the difference in the objective values obtained in every iteration. Note that the average values are obtained under multiple random trials. The result is shown in Fig. 11. One can observe that the objective value converges to an equilibrium level after about 8 iterations. Meanwhile, the convergence gap value reaches the tolerance threshold of the stopping criterion

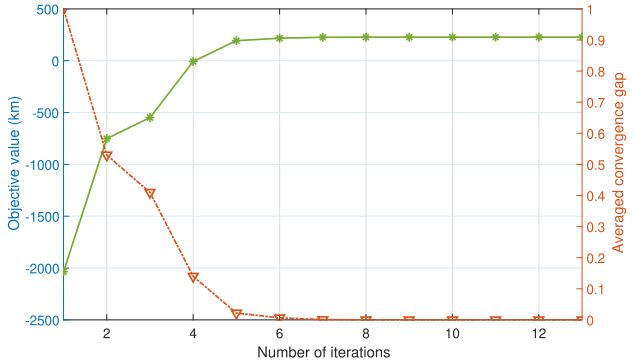

Fig. 11. Convergence of devised algorithm.

in Algorithm 1. This confirms that the devised algorithm is effective in solving the formulated lane-change motion planning problem.

VI. Conclusion

In this paper, we proposed a generic system framework for AV motion planning strategy based on motion prediction and V2V communication. Although the motion planning strategies have been studied in prior work, to the best of our knowledge, this is the first work to incorporate motion planning with the perception system under a unified framework. Meanwhile, we deployed motion prediction and V2V communication techniques to satisfy the real-time interaction between AV and the perception system. The AV lane-change motion planning was then formulated as an MPC programming problem and solved by deriving a related algorithm. In addition, the perception system that is integrated with V2V communication modules enables the motion prediction approach, which further helps AV to learn optimal lane-change motion planning under various traffic conditions. A series of comprehensive simulations demonstrated the effectiveness of the proposed system model under different scenarios. In addition, the robustness of the perception system was validated. Last but not least, the devised algorithm was shown to successfully solve the problem at hand while generating near-optimal solutions.

In future work, we will investigate how to transform the AV motion planning problem into a stochastic problem to model the uncertainties involved in sudden accidents. We will also explore how to implement the function of the V2V communication module into the system model.

References

[1] J. Zhang, F.-Y. Wang, K. Wang, W.-H. Lin, X. Xu, and C. Chen, "Data-driven intelligent transportation systems: A survey," *IEEE Trans. Intell. Transp. Syst.*, vol. 12, no. 4, pp. 1624–1639, Dec. 2011.

[2] Y. Zhang, G. Zhang, R. Fierro, and Y. Yang, "Force-driven traffic simulation for a future connected autonomous vehicle-enabled smart transportation system," *IEEE Trans. Intell. Transp. Syst.*, vol. 19, no. 7, pp. 2221–2233, Jul. 2018.

[3] P. Lin, J. Liu, P. J. Jin, and B. Ran, "Autonomous vehicle-intersection coordination method in a connected vehicle environment," *IEEE Intell. Transp. Syst. Mag.*, vol. 9, no. 4, pp. 37–47, Oct. 2017.

[4] B. Paden, M. Čáp, S. Z. Yong, D. Yershov, and E. Frazzoli, "A survey of motion planning and control techniques for self-driving urban vehicles," *IEEE Trans. Intell. Vehicles*, vol. 1, no. 1, pp. 33–55, Jun. 2016.

[5] L. Ma, J. Xue, K. Kawabata, J. Zhu, C. Ma, and N. Zheng, "Efficient sampling-based motion planning for on-road autonomous driving," *IEEE Trans. Intell. Transp. Syst.*, vol. 16, no. 4, pp. 1961–1976, Aug. 2015.

[6] Y. Huang, H. Wang, A. Khajepour, H. Ding, K. Yuan, and Y. Qin, "A novel local motion planning framework for autonomous vehicles based on resistance network and model predictive control," *IEEE Trans. Veh. Technol.*, vol. 69, no. 1, pp. 55–66, Jan. 2020.

[7] K. Berntorp, T. Hoang, and S. Di Cairano, "Motion planning of autonomous road vehicles by particle filtering," *IEEE Trans. Intell. Vehicles*, vol. 4, no. 2, pp. 197–210, Jun. 2019.

[8] Y. Jeong and K. Yi, "Target vehicle motion prediction-based motion planning framework for autonomous driving in uncontrolled intersections," *IEEE Trans. Intell. Transp. Syst.*, vol. 22, no. 1, pp. 168–177, Jan. 2021.

[9] L. Claussmann, M. Revilloud, D. Gruyer, and S. Glaser, "A review of motion planning for highway autonomous driving," *IEEE Trans. Intell. Transp. Syst.*, vol. 21, no. 5, pp. 1826–1848, May 2020.

[10] P. Nilsson, L. Laine, and B. Jacobson, "A simulator study comparing characteristics of manual and automated driving during lane changes of long combination vehicles," *IEEE Trans. Intell. Transp. Syst.*, vol. 18, no. 9, pp. 2514–2524, Sep. 2017.

[11] J. Guo, S. Cheng, and Y. Liu, "Merging and diverging impact on mixed traffic of regular and autonomous vehicles," *IEEE Trans. Intell. Transp. Syst.*, vol. 22, no. 3, pp. 1639–1649, Mar. 2021.

[12] J. Suh, H. Chae, and K. Yi, "Stochastic model-predictive control for lane change decision of automated driving vehicles," *IEEE Trans. Veh. Technol.*, vol. 67, no. 6, pp. 4771–4782, Jun. 2018.

[13] Y. Liu, X. Wang, L. Li, S. Cheng, and Z. Chen, "A novel lane change decision-making model of autonomous vehicle based on support vector machine," *IEEE Access*, vol. 7, pp. 26543–26550, 2019.

[14] C. Wang, Q. Sun, Z. Li, H. Zhang, and K. Ruan, "Cognitive competence improvement for autonomous vehicles: A lane change identification model for distant preceding vehicles," *IEEE Access*, vol. 7, pp. 83229–83242, 2019.

[15] Y. Chen, C. Hu, and J. Wang, "Motion planning with velocity prediction and composite nonlinear feedback tracking control for lane-change strategy of autonomous vehicles," *IEEE Trans. Intell. Vehicles*, vol. 5, no. 1, pp. 63–74, Mar. 2020.

[16] N. Lu, N. Cheng, N. Zhang, X. Shen, and J. W. Mark, "Connected vehicles: Solutions and challenges," *IEEE Internet Things J.*, vol. 1, no. 4, pp. 289–299, Aug. 2014.

[17] A. Eskandarian, C. Wu, and C. Sun, "Research advances and challenges of autonomous and connected ground vehicles," *IEEE Trans. Intell. Transp. Syst.*, vol. 22, no. 2, pp. 683–711, Feb. 2021.

[18] E. Arnold, M. Dianati, R. de Temple, and S. Fallah, "Cooperative perception for 3D object detection in driving scenarios using infrastructure sensors," *IEEE Trans. Intell. Transp. Syst.*, vol. 23, no. 3, pp. 1852–1864, Mar. 2022.

[19] E. E. Marvasti, A. Raftari, A. E. Marvasti, Y. P. Fallah, R. Guo, and H. Lu, "Cooperative LIDAR object detection via feature sharing in deep networks," in *Proc. IEEE 92nd Veh. Technol. Conf. (VTC-Fall)*, Nov. 2020, pp. 1–7.

[20] M. Ambrosin *et al.*, "Object-level perception sharing among connected vehicles," in *Proc. IEEE Intell. Transp. Syst. Conf. (ITSC)*, Oct. 2019, pp. 1566–1573.

[21] Z. Zhang, S. Wang, Y. Hong, L. Zhou, and Q. Hao, "Distributed dynamic map fusion via federated learning for intelligent networked vehicles," in *Proc. IEEE Int. Conf. Robot. Autom. (ICRA)*, May 2021, pp. 953–959.

[22] S. Wang *et al.*, "Federated learning connected autonomous vehicle: Perception system design and implementation," *IEEE Netw.*, 2022.

[23] S. Pagadarai, B. A. Lessard, A. M. Wyglinski, R. Vuyyuru, and O. Altintas, "Vehicular communication: Enhanced networking through dynamic spectrum access," *IEEE Veh. Technol. Mag.*, vol. 8, no. 3, pp. 93–103, Sep. 2013.

[24] T. Zhang, Y. Xu, S. Wang, M. Wen, and R. Wang, "On secure degrees of freedom of the MIMO interference channel with local output feedback," *IEEE Internet Things J.*, vol. 8, no. 20, pp. 15334–15348, Oct. 2021.

[25] C. Edwards, J. Hankey, R. Kiefer, D. Grimm, and N. Leask, "Understanding driver perceptions of a vehicle to vehicle (V2V) communication system using a test track demonstration," *SAE Int. J. Passenger Cars-Mech. Syst.*, vol. 4, no. 1, pp. 444–461, Apr. 2011.

[26] X. Han *et al.*, "Reliability-aware joint optimization for cooperative vehicular communication and computing," *IEEE Trans. Intell. Transp. Syst.*, vol. 22, no. 8, pp. 5437–5446, Aug. 2021.

[27] D. D. Yoon, B. Ayalew, and G. G. M. N. Ali, "Performance of decentralized cooperative perception in V2V connected traffic," *IEEE Trans. Intell. Transp. Syst.*, early access, Mar. 26, 2021, doi: 10.1109/TITS.2021.3063107.

[28] R. Fukatsu and K. Sakaguchi, "Millimeter-wave V2V communications with cooperative perception for automated driving," in *Proc. IEEE 89th Veh. Technol. Conf. (VTC-Spring)*, Apr. 2019, pp. 1–5.

[29] Z. He, L. Zheng, L. Lu, and W. Guan, "Erasing lane changes from roads: A design of future road intersections," *IEEE Trans. Intell. Vehicles*, vol. 3, no. 2, pp. 173–184, Jun. 2018.

[30] R. Dang, J. Ding, B. Su, Q. Yao, Y. Tian, and K. Li, "A lane change warning system based on V2V communication," in *Proc. 17th Int. IEEE Conf. Intell. Transp. Syst. (ITSC)*, Oct. 2014, pp. 1923–1928.

[31] T. Li *et al.*, "A cooperative lane change model for connected and automated vehicles," *IEEE Access*, vol. 8, pp. 54940–54951, 2020.

[32] P. A. Lopez *et al.*, "Microscopic traffic simulation using SUMO," in *Proc. IEEE Int. Conf. Intell. Transp. Syst. (ITSC)*, Mar. 2018, pp. 2575–2582.

[33] A. Dosovitskiy, G. Ros, F. Codevilla, A. Lopez, and V. Koltun, "CARLA: An open urban driving simulator," in *Proc. 1st Annu. Conf. Robot Learn.*, in Proceedings of Machine Learning Research, vol. 78, S. Levine, V. Vanhoucke, and K. Goldberg, Eds., Nov. 2017, pp. 1–16.

[34] ASTM International. (Dec. 2017). *Road Standards and Paving Standards*. [Online]. Available: https://www.astm.org/Standards/road-and-paving-standards.html

[35] S. Dang, O. Amin, B. Shihada, and M.-S. Alouini, "What should 6G be?" *Nature Electron.*, vol. 3, no. 1, pp. 20–29, Jan. 2020.

[36] National Highway Traffic Safety Administration. (Apr. 2017). *Federal Motor Vehicle Safety Standards; V2V Communications*. [Online]. Available: https://www.federalregister.gov/documents/2017/01/12/2016-31059/federal-motor-vehicle-safety-standards-v2v-communications

[37] C. Goodin, D. Carruth, M. Doude, and C. Hudson, "Predicting the influence of rain on LIDAR in ADAS," *Electronics*, vol. 8, no. 1, pp. 1–9, Jan. 2019.

[38] Y. Sun, D. Li, X. Wu, and Q. Hao, "Visual perception based situation analysis of traffic scenes for autonomous driving applications," in *Proc. IEEE 23rd Int. Conf. Intell. Transp. Syst. (ITSC)*, Sep. 2020, pp. 1–7.

[39] J. J. Q. Yu, C. Markos, and S. Zhang, "Long-term urban traffic speed prediction with deep learning on graphs," *IEEE Trans. Intell. Transp. Syst.*, early access, Apr. 9, 2021, doi: 10.1109/TITS.2021.3069234.

[40] T. Peng *et al.*, "Lane-change model and tracking control for autonomous vehicles on curved highway sections in rainy weather," *J. Adv. Transp.*, vol. 2020, no. 11, pp. 1–15, Nov. 2020.

[41] F. Bella and R. Russo, "A collision warning system for rear-end collision: A driving simulator study," *Proc.-Social Behav. Sci.*, vol. 20, pp. 676–686, Aug. 2011.

[42] Z.-Q. Zhao, P. Zheng, S.-T. Xu, and X. Wu, "Object detection with deep learning: A review," *IEEE Trans. Pattern Anal. Mach. Intell.*, vol. 30, no. 11, pp. 3212–3232, Nov. 2019.

[43] Tesla. (Mar. 2021). *Model 3*. [Online]. Available: https://www.tesla.com/model3.

[44] J. Q. James and A. Y. S. Lam, "Autonomous vehicle logistic system: Joint routing and charging strategy," *IEEE Trans. Intell. Transp.*, vol. 19, no. 7, pp. 2175–2187, Jul. 2018.

[45] L. Sun, C. Peng, W. Zhan, and M. Tomizuka, "A fast integrated planning and control framework for autonomous driving via imitation learning," in *Proc. Dyn. Syst. Control Conf.*, Sep. 2018, pp. 1–11.

[46] A. Ghasemzadeh and M. M. Ahmed, "Drivers' lane-keeping ability in heavy rain: Preliminary investigation using SHRP 2 naturalistic driving study data," *Transp. Res. Rec., J. Transp. Res. Board*, vol. 2663, no. 1, pp. 99–108, Jan. 2017.

[47] A. A. Kordani, O. Rahmani, A. S. A. Nasiri, and S. M. Boroomandrad, "Effect of adverse weather conditions on vehicle braking distance of highways," *Civil Eng. J.*, vol. 4, no. 1, pp. 46–57, Feb. 2018.

Shiyao Zhang (Member, IEEE) received the B.S. degree (Hons.) in electrical and computer engineering from Purdue University, West Lafayette, IN, USA, in 2014, the M.S. degree in electrical engineering (electric power) from the University of Southern California, Los Angeles, CA, USA, in 2016, and the Ph.D. degree from The University of Hong Kong, Hong Kong, China. He is currently a Post-Doctoral Research Fellow with the Academy for Advanced Interdisciplinary Studies, Southern University of Science and Technology. His research interests include smart energy systems, intelligent transportation systems, optimization theory and algorithms, and deep learning applications.

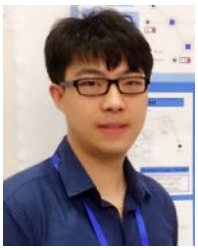

Shuai Wang (Member, IEEE) received the Ph.D. degree in electrical and electronic engineering from The University of Hong Kong (HKU) in 2018. From 2018 to 2019, he was a Post-Doctoral Fellow at HKU. From 2019 to 2021, he was a Research Assistant Professor at the Southern University of Science and Technology (SUSTech). He is currently an Associate Professor with the Shenzhen Institute of Advanced Technology (SIAT), Chinese Academy of Sciences. He has published more than 30 articles in IEEE top journals and more than 20 papers in IEEE flagship conferences. His research interests include autonomous driving, edge intelligence, optimization, and communication. He has received the Best Paper Awards from IEEE ICC in 2020 and IEEE SPCC in 2021.

Shuai Yu (Member, IEEE) received the B.S. degree from the Nanjing University of Posts and Telecommunications (NJUPT), Nanjing, China, in 2009, the M.S. degree from the Beijing University of Posts and Telecommunications (BUPT), Beijing, China, in 2014, and the Ph.D. degree from University Pierre and Marie Curie (now Sorbonne Universite), Paris, France, in 2018. He is currently an Associate Professor with Sun Yat-sen University, Guangzhou, China. His research interests include edge computing, mobile computing, machine learning, and space-air-ground integrated networks.

James J. Q. Yu (Senior Member, IEEE) received the B.Eng. and Ph.D. degrees in electrical and electronic engineering from The University of Hong Kong, Hong Kong, in 2011 and 2015, respectively. He was a Post-Doctoral Fellow at The University of Hong Kong from 2015 to 2018. He is currently an Assistant Professor at the Department of Computer Science and Engineering, Southern University of Science and Technology, Shenzhen, China; and an Honorary Assistant Professor at the Department of Electrical and Electronic Engineering, The University of Hong Kong. He also serves as the Chief Research Consultant for GWGrid Inc., Zhuhai; and Fano Labs, Hong Kong. His work is now mainly on forecasting and decision making of future transportation systems and basic artificial intelligence techniques for industrial applications. His general research interests are in smart city and urban computing, deep learning, intelligent transportation systems, and smart energy systems. He was ranked World's Top 2% Scientists of 2019 and 2020 by Stanford University. He is an Editor of the *IET Smart Cities* journal.

Miaowen Wen (Senior Member, IEEE) received the Ph.D. degree from Peking University, Beijing, China, in 2014.

From 2019 to 2021, he was with the Department of Electrical and Electronic Engineering, The University of Hong Kong, Hong Kong, as a Post-Doctoral Research Fellow. He is currently a Professor with the South China University of Technology, Guangzhou, China. He has published two books and more than 150 journal articles. His research interests include a variety of topics in the areas of wireless and molecular communications. He was a recipient of the IEEE ComSoc Asia–Pacific Outstanding Young Researcher Award in 2020 and the four Best Paper Awards from the IEEE ITST'12, the IEEE ITSC'14, the IEEE ICNC'16, and the IEEE ICCT'19. He was the Winner in Data Bakeoff Competition (Molecular MIMO) at IEEE Communication Theory Workshop (CTW) 2019, Selfoss, Iceland. He has served as a Guest Editor for the IEEE JOURNAL ON SELECTED AREAS IN COMMUNICATIONS and the IEEE JOURNAL OF SELECTED TOPICS IN SIGNAL PROCESSING. He is serving as an Editor for the IEEE TRANSACTIONS ON COMMUNICATIONS, the IEEE TRANSACTIONS ON MOLECULAR, BIOLOGICAL, AND MULTI-SCALE COMMUNICATIONS, and the IEEE COMMUNICATIONS LETTERS.